Available online at www.sciencedirect.com

ScienceDirect

Ceramics International 40 (2014) 4673–4679

CERAMICS INTERNATIONAL

www.elsevier.com/locate/ceramint

A simple microwave-assisted combustion synthesis and structural, optical and magnetic characterization of ZnO nanoplatelets

Yüksel Köseoğlu[a,b,*]

[a]Department of Physics, Fatih University, Buyukcekmece 34500, Istanbul-Turkey
[b]Faculty of Engineering and Natural Sciences, Suleyman Demirel University, 040900 Almaty, Kazakhstan

Received 20 June 2013; received in revised form 22 August 2013; accepted 2 September 2013
Available online 8 September 2013

Abstract

A simple microwave-assisted combustion route was used first time for the preparation of nanocrystalline ZnO nanoplatelets using dissolution of zinc nitrate as the oxidant and glycin as fuel. The structure, morphology and composition of the as-prepared samples were investigated by X-ray powder diffraction (XRD), Scanning electron microscopy (SEM) and Energy dispersive X-ray spectra (EDX). The XRD results confirmed the formation of single phase hexagonal wurtzite structure of ZnO and SEM pictures indicated that the sample includes the nanostructured nanoplatelets with the porous surface of the products. The optical properties were determined by a UV–vis spectrophotometer and the results showed that the as prepared ZnO nanoplatelets have larger band gap of 3.06 eV. Vibrating sample magnetometer (VSM) was used for the magnetic property investigations and ZnO nanoplatelets indicated room temperature ferromagnetism which is intrinsic in nature and attributed to oxygen and/or Zn deficiencies as found in EDX results.

Keywords: Diluted magnetic semiconductors; Microwave combustion; RT ferromagnetism; ZnO nanoplatelets; SEM

1. Introduction

Diluted magnetic semiconductors (DMS) play a major role as attractive research materials in spintronics applications due to their potential as spin polarized carrier sources in spin polarized electronics. Due to combined effect of magnetic and semiconducting behaviors, ferromagnetic diluted semiconductors in which the spin degree of freedom is added to charge, exhibit interesting properties like magnetic, opto-electronic, magneto-electronic, magneto-optical and spintronic. For spintronics application the room-temperature-ferromagnetism (RTFM) is important. The materials representing RTFM properties are generally obtained by replacing magnetic ions (3d transition metal (TM) ions such as Ni, V, Cr, Mn, Fe, Co, Cu, etc.) with a small part of non magnetic semiconductor atoms [1–4].

Nanostructured zinc oxide (ZnO) is technologically very attractive nanomaterial to be used in various application areas with its wide direct band gap of 3.37 eV and large exciton binding energy of 60 meV. It has wurtzite structure and unique electronic, optical, catalytic and acoustic properties. Nanostructured ZnO materials have potential application in field effect transistors, flat panel displays, spin light emitting diodes, solar cells, sensors, ultraviolet nanolasers, etc. [4–11]. It is commonly known that by adding certain kind of impurities to semiconductors, it is possible to optimize optical, magnetic and electrical properties of the materials.

Based on theoretical studies for RTFM properties achieved in TM doped ZnO, a lot of experimental work has been performed and experimentally RTFM has been observed in nanoparticles, nanorods, nanoflakes and thin films of TM doped ZnO structures [4–8,12].

While the researchers are trying to explain RTFM in doped DMS materials, they have observed ferromagnetism in undoped semiconducting nanomaterials [2,13–17]. The ferromagnetism observed in undoped ZnO structures is attributed to some kind of defects such as oxygen vacancy (*Vo*) related defects and/or Zn site defects [1,6,15,17,18].

*Correspondence address : Department of Physics, Fatih University, Buyukcekmece 34500, Istanbul-Turkey. Tel.: +90 212 866 3300; fax: +90 212 866 3402.
E-mail address: yukselk@fatih.edu.tr

0272-8842/$ - see front matter © 2013 Elsevier Ltd and Techna Group S.r.l. All rights reserved.
http://dx.doi.org/10.1016/j.ceramint.2013.09.008

Previous researhes on ZnO have revealed that the optical, electronic and magnetic properties of ZnO strongly depend on its microstructure such as; crystal size, morphology, specific surface and crystalline density [19–21]. Therefore many kinds of ZnO nanostructures such as nanoparticles, nanowires, nanoisland, hollow microspheres, nanoporous belts, nanoplates, nanotubes, etc. have been synthesized by using several numbers of methods including combustion, sol–gel processing, chemical precipitation, hydrothermal, mechanical milling, organometallic synthesis, spray pyrolysis, thermal evaporation, mechanochemical synthesis etc. [4,18,22–34]. The combustion method becomes the most efficient choice among these methods in case of large scale economical production of nanomaterials [35,36]. Furthermore when the combustion is assisted by microwave radiation called as microwave assisted combustion as in this work, it becomes faster to synthesize and more cost effective compared to the previous methods.

Generally, conventional heating synthesis methods are used in the processes of combustion. In all conventional means for heating reaction mixtures, heating proceeds from the surface of the solution, usually the inside surface of the reaction vessel and the mixture must be in physical contact with a surface that is at a higher temperature than the rest of the mixture. Microwave irradiation is becoming an increasingly popular method of synthesis. It offers a clean, cheap, and convenient method of heating which often results in higher yields and shorter reaction times. The heating mechanism, however, is fundamentally different in microwave processing from the conventional processing methods. In a microwave assisted combustion synthesis, due to the interaction of microwaves with the material, the heat is generated within the sample itself. In this method, the microwave energy heats the material on a molecular level leading to a uniform heating with the matter from bulk to the surface. In this method, the generation of heat is governed by the rapid kinetics of the dipole moments of the molecules. It is clearly understood that in the microwave combustion method, during the reaction process, the molecular dipoles are induced to oscillate by microwave. This oscillation causes higher rate of molecular collision generating enormous amount of heat. Therefore, the temperature distribution is homogeneous inside the solution and transferred to the materials interior, making explosion reaction followed by vigorous evolution of gases to form nanostructures. Also, in the microwave assisted combustion synthesis, the heating is usually achieved within few minutes, which gives early phase formation and fine particle size of the desired sample. Furthermore, in microwave assisted synthesis, the reaction time is short and the complex equipment is not needed in this method, making this technique very attractive. Therefore, it is possible to control both kinetic and thermodynamic factors of the chemical reactions using microwave in the combustion processes. Hence this microwave assisted combustion method offers several advantages like simple reaction process, forming a chemically homogeneous composition, inexpensive, low energy loss, high-production efficiency, high purity and non-toxic products [35–40].

The main advantages of microwave assisted combustion synthesis are uniform heating of the reaction mixture, generation of localized instantaneous high temperatures at the reaction sites, shorter reaction times, selective formation of specific morphology, reduced energy consumption and higher product yields. Due to these advantages, uniformly dispersed and better crystalline nanomaterials could be synthesized in one-pot reaction within a short period. So, the microwave induced combustion method is a simple and fast method for the production of ZnO nanoflakes with no need for complicated treatments and/or expensive materials.

In the present work, ZnO nanoplatelets were synthesized first time by a simple microwave assisted combustion method which is very fast and cost effective method compared to the other methods. The synthesized sample was characterized by several techniques such as X-ray diffraction (XRD), scanning electron microscopy (SEM), energy-dispersive X-ray spectroscopy (EDX), ultraviolet–visible spectroscopy (UV–vis absorbance), Fourier transform infrared spectroscopy (FT-IR), vibrating sample magnetometer (VSM) and discussed with details in results and discussion part.

2. Experimental

2.1. Procedure

Zinc nitrate hexahydrate ($Zn(NO_3)_2 \cdot H_2O$, $> 99\%$), and urea ($CO(NH_2)_2$) were purchased from Sigma-Aldrich and used without further purification. An appropriate ratio of zinc nitrate as oxidant and urea as a fuel, were dissolved in proper amounts of deionized water by stirring with magnetic stirrer well for 30 min and the mixture is poured into a crucible. And then the crucible is placed in a kitchen-type microwave oven operating at 800 W for 20 min till the precursor solution mixture decomposes. The solution initially boils then undergoes dehydration followed by decomposition with the evolution of large fumes in the form of smoke. This spontaneous combustion vaporized the solution mixture. When the solution reaches the point of spontenous combustion, it begins to release heat by burning and turns into solid powder, thus forming the desired phase.

2.2. Materials characterization

X-ray powder diffraction (XRD) analysis was conducted on a Rigaku Smart Lab Diffractometer operated at 40 kV and 35 mA using Cu K_α radiation for the structural characterization and phase identification. Field Emission Scanning Electron Microscope (FE-SEM, JEOL 7001 FE) was used in order to investigate the nanostructure and morphology of the samples. Samples were sputtered on cupper substrate and then coated with gold-palladium to make it conductive prior to SEM analysis.

For optical property investigations, the UV–vis absorbance spectrum was obtained by using Thermo Fisher Scientific EVO300 PC model spectrophotometer. Magnetic measurements were performed by using a Quantum Design Vibrating

sample magnetometer (QD-VSM). The samples were measured between ± 10 kOe at room temperature and 10 K. Zero field cooling (ZFC) and field cooling (FC) measurements were carried out at 50 Oe and the blocking temperature was determined from the measurements.

3. Results and discussion

3.1. XRD analysis

Fig. 1 shows XRD pattern of the prepared ZnO nanopowders. After observing the XRD graph, it can easily be seen that all the diffraction peaks ((100), (002), (101), (102), (110), (103), (200), (112), and (201)) in the pattern can be perfectly indexed to the hexagonal wurtzite structure of pure ZnO which is identical to pure ZnO wurtzite structure according to "JCPDS no. 01-089-7102". The diffraction peaks are narrower and sharp indicating the good cryatallinity of the as prepared ZnO powder. Based on this XRD pattern, no obvious impurity phases such as ZnO_2 were observed.

The average crystallite size of the sample was evaluated by measuring the broadening of the XRD peaks using the Scherrer equation [37]

$$D = \left(\frac{180}{\pi}\right)\left(\frac{K\lambda}{\cos(\theta)\sqrt{\beta^2 - s^2}}\right) \quad (1)$$

where D is the crystallite size, λ is the wavelenght of the CuK_α radiation (1.5402 A), K is a constant (0.9), s is the instrumental broadening, β is the full-width at half-maximum and θ is the Bragg angle where the most intense peak occured (the (101) peak in this case). The calculated crystallite size of ZnO powders is found to be 33.54 nm.

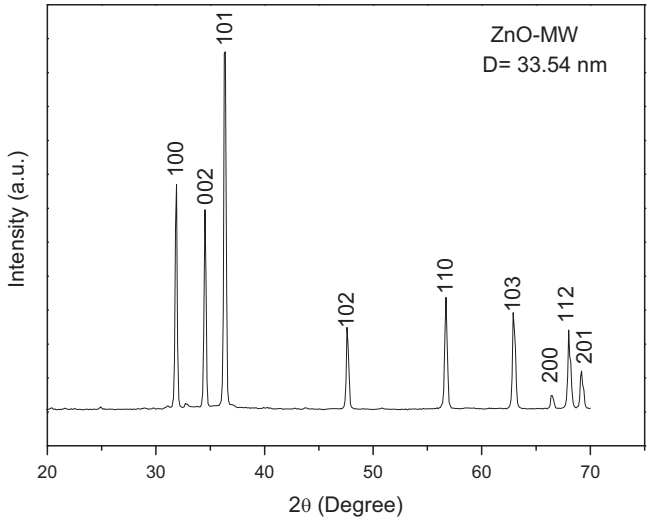

Fig. 1. XRD pattern obtained from as synthesized ZnO nanoplatelets.

In this study, the lattice parameters a and c of the synthesized samples were calculated via the following relation which is used for hexagonal systems [36]

$$\frac{4\sin^2\theta}{\lambda^2} = \frac{4}{3}\left(\frac{h^2+hk+k^2}{a^2}\right) + \frac{l^2}{c^2} \quad (2)$$

where θ is the Bragg angle, a and c are lattice constants, h,k,l are Miller indices, and λ is the wavelenght of X-ray used (1.5402 A).

After choosing proper peaks ((110) for a and (001) for c) following equations are deduced for lattice constants a and c

$$a = \frac{\lambda\sqrt{(h^2+hk+k^2)}}{\sqrt{3}\ \sin\ \theta} \quad (3)$$

and

$$c = \frac{\lambda l}{2\ \sin\ \theta} \quad (4)$$

Furthermore, the lattice volume was also evaluated by the formula given below

$$V = 0.866a^2c \quad (5)$$

The calculated results are represented in Table 1.

3.2. SEM measurements

Morphology of the as prepared sample is characterized by scanning electron microscopy (SEM) as shown in Fig. 2. As it is seen from SEM pictures the ZnO samples consist of nanoplatelets and there is a small agglomeration between the platelets. There is a stack of nanoplatelets. If the pictures are magnified, it can be seen that each nanoplatelet consists of fine nanoparticles. As it is seen from the magnified SEM picture, the plates consist of nanoparticles with sizes of 20–40 nm which are stacked to produce the plates.

In addition, EDX spectrum (Fig. 3) confirms that as prepared ZnO samples are composed of zinc and oxygen elements with very small amounts of nitrogen impurity element which make a small amount of N doped ZnO. The peak at 0.9 keV (close to the Zn peak) comes from copper substrate, the peak at 2.15 keV comes from gold due to Au–Pd coating, and the peak at 2.9 keV (minor) on the EDS spectrum comes from palladium due to Au–Pd coating. Also small amount of nitrogen content in the EDS spectrum indicates the formation of N substituted ZnO phase but the ratio of NZnO/ZnO is very small. Gold and paladium peaks in the EDX spectrum comes from the Au–Pd coating done on the sample to make it conducting for SEM measurements.

Table 1
Structural, magnetic and optical parameters found for ZnO nanoplatelets.

Sample	*hkl*	*D*(nm)	*hkl*	*a*=*b* (A)	*hkl*	*c* (A)	*V* (A^3)	M_s (emu/g)	H_c (Oe)	E_g (eV)
ZnO	101	33,54	110	3,2436	002	5,1932	47.32	0.032	60	3.09

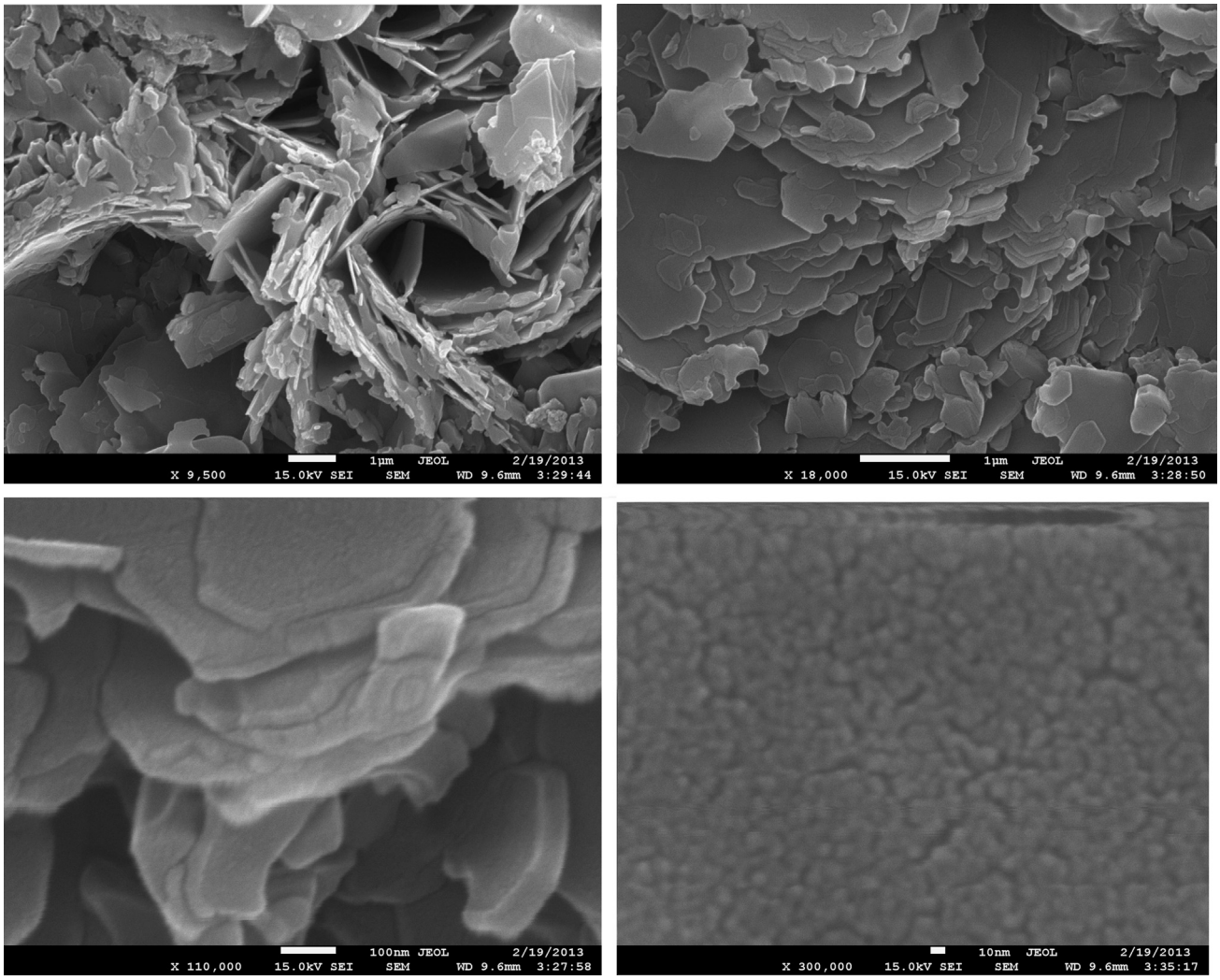

Fig. 2. SEM micrographs with different magnifications of ZnO nanoplatelets synthesized by the microwave-assisted combustion method.

3.3. Optical study

UV–vis absorbance spectrum of the as synthesized samples is shown in Fig. 4. For nanostructured DMS materials, the optical band gap energy (E_g) is an important parameter for the use of nanostructured DMS materials in special applications. It is known that band gap energy of semiconducting materials may change with the size and shape of the particles or defects on the particles and also strongly dependent upon the synthesis methods used [36].

The UV–vis absorbance of the samples was recorded and the energy band gap, E_g value of ZnO nanoplatelets was determined as 3.09 eV by using the folowing relation [41]:

$$(\alpha E) = A(E - E_g)^n \tag{6}$$

where A is an energy-independent constant, E_g is the direct energy band gap, α is the absorption coefficient, E is the photon energy and n is an index that characterizes the optical absorption process and it is theoretically equal to 1/2 and 2 for direct and indirect transitions, respectively.

The the photon energy can be approximated by the following relationship:

$$E = \frac{hc}{\lambda} = \frac{1240}{\lambda}\ ev \tag{7}$$

where λ is the wavelength in nanometers.

The $(\alpha E)^2$ versus E for the samples was plotted as shown in inset of Fig. 4. and the energy band gap E_g value is given in Table 1.

3.4. Magnetization measurements

The magnetization measurements were carried out using vibrating sample magnetometer (VSM). The room temperature field dependent magnetization curve (M–H) of the sample is represented in Fig. 5. As it is seen from the figure, M–H curve has an s-shaped curve with a coercivity of 60 Oe which indicates that the ZnO nanoparticles sythesized by microwave assisted combustion method exhibit a typical ferromagnetic behavior at room temperature. The saturation magnetization M_s of the sample is measured as 3×10^{-3} emu/g which is

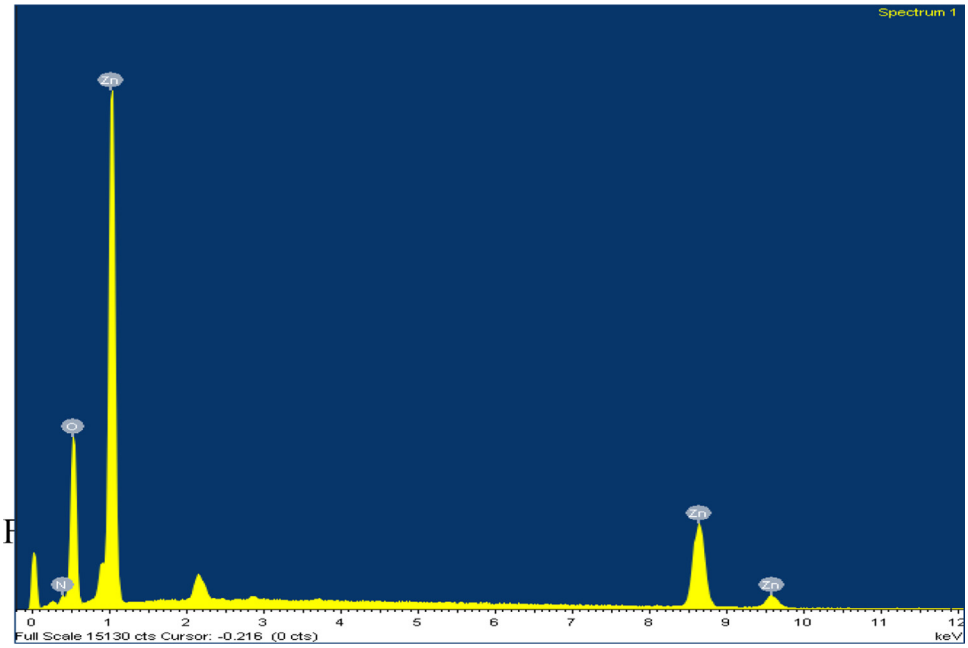

Fig. 3. EDX pattern obtained for ZnO nanoplatelets.

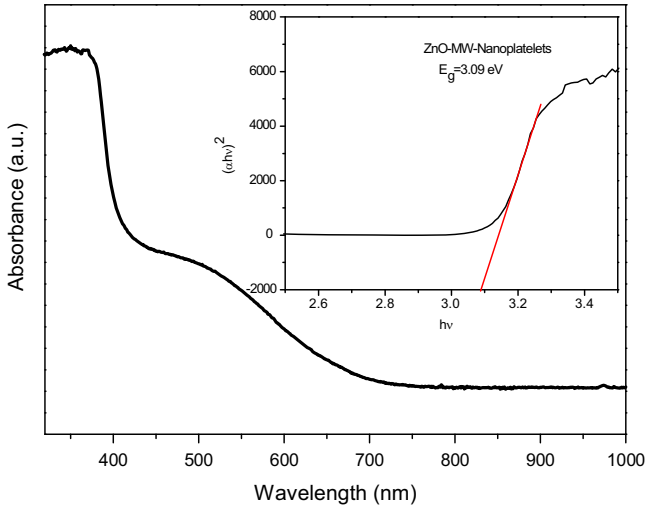

Fig. 4. UV–vis absorption spectrum of ZnO nanoplatelets synthesized by the microwave assisted combustion method.

larger than that of the nanoparticles synthesized by sol–gel calcination process [1], nanoparticles synthesized by the wet chemical method [42], nanoparticles synthesized by pulsed laser deposition [43], nanoparticles prepared by the sol–gel method [44], nanoparticles prepared by microwave plasma process [17] and nanorods synthesized by the hydrothermal method [45].

In order to obtain more detailed information on ferromagnetic behavior of ZnO nanoparticles ttypical temperature dependent zero field cooled (ZFC) and field cooled (FC) magnetization measurements were done at 100 Oe applied field and the temperature variation of the magnetization is shown in Fig. 6. For ZFC measurements, the sample was first cooled down to 10 K in the absence of an applied field and the magnetization of the sample was measured in the temperature range from 400 K to 10 K. In contrast, FC measurements were carried out at a constant applied magnetic field of 100 Oe between the same temperature range.

As seen from Fig. 6, both ZFC and FC magnetizations of the sample show nonzero magnetization at all measuring temperatures which is consistant with *M–H* curve. While ZFC magnetization is gradually decreasing with temperature decrease, the FC magnetization is increasing slightly as expected for metallic compounds. FC and ZFC curves are apart from each other with nozero values indicating that the sample shows ferromagnetic behavior at all measuring temperatures. The transition temperature (Curie temperature, T_C) was noticed to be above 400 K. The ZFC and FC magnetic properties of the sample appear to be characteristic of ferromagnetic behavior and rule out paramagnetic and/or antiferromagnetic nature of ZnO sample. The mechanism responsible for ferromagnetic behavior of ZnO samples is still contraversial. But, since XRD and EDX measurements indicate no impurity phases, the structural characterizations rule out the ferromagnetism due to impurity phases in our sample. The ferromagnetic behavior in our sample can be attributed to uncontrolled formation of lattice defects generating carriers that mediate ferromagnetic behavior as observed for earlier studies [46–48].

The ferromagnetic behavior on ZnO sample prepared by the microwave-assisted combustion method may come from the exchange interaction between localized spin moments resulting from the oxygen vacancies at the surface of nanoplatelets. Generally, native point defects such as oxygen vacancies are common in ZnO nanoparticles giving rise to ferromagnetic behavior [36,46–48]. Our sample exhibit higher magnetization value as compared with ZnO nanostructured samples produced by different methods, which can be attributed to the formation of higher amounts of lattice defects (oxygen vacancies) as a

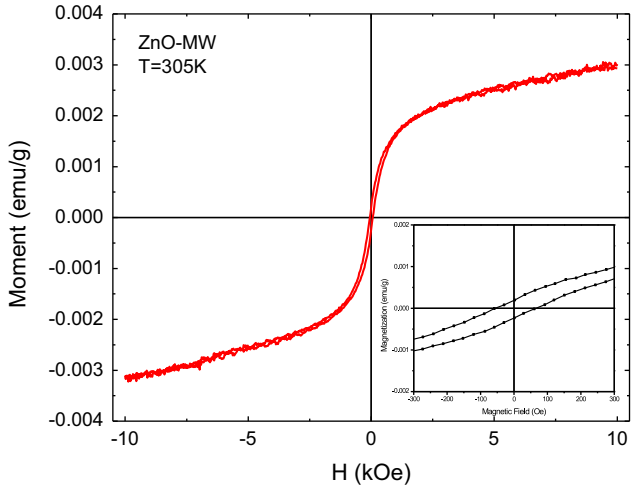

Fig. 5. Room temperature *M–H* curve obtained from ZnO nanoparticles. The inset shows the enlarged view *M–H* curve.

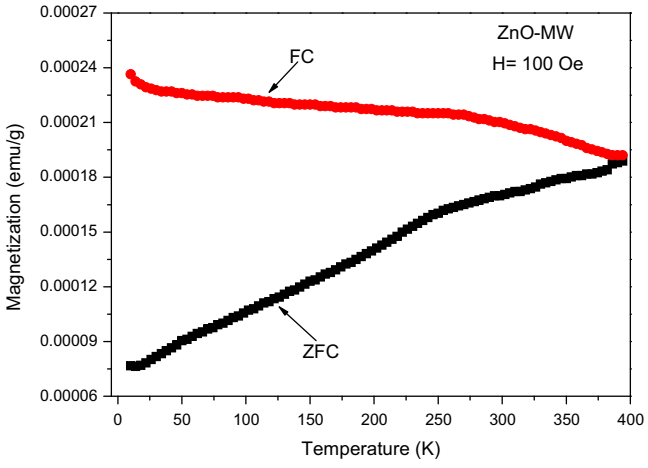

Fig. 6. Temperature dependent FC and ZFC magnetization.

result of oriented attachment among nanocrystals. Higher amounts of lattice defects may come from different synthesis conditions compared with other methods.

Also the difference between M_{FC} and M_{ZFC} curves indicated in Fig. 7. The difference between M_{FC} and M_{ZFC} decreases with temperature and it is nonzero at all measuring temperatures. This means that, ferromagnetic property of the sample can be observed at all measuring measurement temperatures which agrees with the *M–H* results.

4. Conclusion

Ferromagnetic ZnO nanoplatelets have been successfully prepared first time via a microwave-assisted combustion route. The structural, morphological, optical and magnetic properties of as prepared samples have been investigated. X-ray diffraction pattern confirms that ZnO nanoplatelets have polycrystalline nature with hexagonal wurtzite structure without any impurity phase. The crystallite size of ZnO is found as 33.54 nm. SEM micrographs indicated that ZnO sample

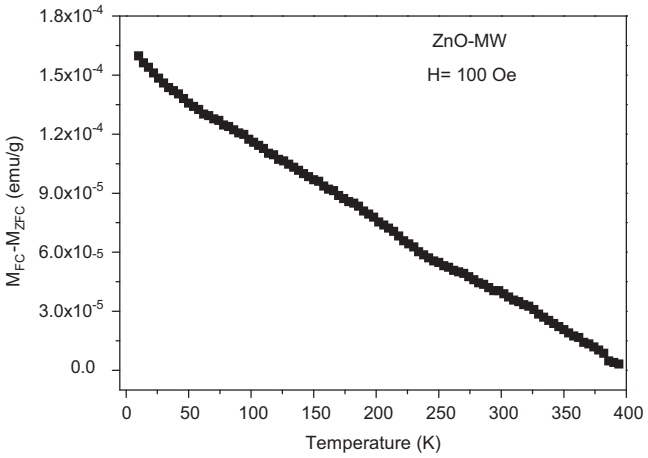

Fig. 7. Temperature dependence of the difference between M_{FC} and M_{ZFC} magnetizations of the ZnO nanoplatelets.

consists of nanoplatelets with small aggregation and each nanoplate also consists of fine nanoparticles. The optical studies confirm that the ZnO nanoplatelets have semiconducting properties with a direct energy band gap of 3.09 eV. VSM measurements have revealed that ZnO nanoplatelets have room temperature ferromagnetic behavior with a coercivity of 60 Oe. FC and ZFC measurements have indicated that the sample is ferromagnetic at all measuring temperatures and it has a Curie temperature above 400 K. The ferromagnetism of ZnO nanoplatelets is assigned to oxygen and/or Zn defects.

References

[1] Y.Z. Zang, E. Xie, Nature of room-temperature ferromagnetism from undoped ZnO nanoparticles, Applied Physics A 99 (2010) 955.
[2] A. Wolf, D.D. Awschalom, R.A. Buhrman, J.M. Daughton, S. von Molnar, M.L. Roukes, A.Y. Chtchelkanova, D.M. Treger, Spintronics: a spin-based electronics vision for the future, Science 294 (2001) 1488–1495.
[3] T. Dietl, H. Ohno, F. Matsukura, J. Cibert, D. Ferrand, Zener model description of ferromagnetism in zinc-blende magnetic semiconductors, Science 287 (2000) 1019–1022.
[4] Yüksel Köseoğlu, Enhanced ferromagnetic properties of Co-doped ZnO DMS nanoparticles, Journal of Superconductivity and Novel Magnetism 26 (2013) 485–489.
[5] Y. Ohno, D.K. Young, B. Beschoten, F. Matsukura, H. Ohno, D. D. Awschalom, Electrical spin injection in a ferromagnetic semiconductor heterostructure, Nature 402 (1999) 709.
[6] D. Maouche, P. Ruterana, L. Louail, Carrier-mediated ferromagnetism in N co-doped (Zn, Mn) O-based diluted magnetic semiconductors, Physics Letters A 365 (2007) 231–234.
[7] Y.Z. Peng, T. Liew, T.C. Chong, C.W. An, W.D. Song, Anomalous hall effect and origin of magnetism in Zn1 − *x*Co*x*O thin films at low Co content, Applied Physics Letters 88 (2006) 192110/1–192110/3.
[8] R. Elilarassi, G. Chandrasekaran, Structural, optical and magnetic properties of nanoparticles of ZnO:Ni DMS prepared by the sol–gel method, Materials Chemistry and Physics 123 (2010) 450–455.
[9] S. Guo, Z. Du, Infuence of defects on magnetism of Co-doped ZnO, Journal of Magnetism and Magnetic Materials 324 (2012) 782–785.
[10] Y. Peng, D. Huo, H. He, Y. Li, L. Li, H. Wang, Z. Qian, Characterization of ZnO:Co particles prepared by hydrothermal method for room temperature magnetism, Journal of Magnetism and Magnetic Materials 324 (2012) 690–694.

[11] L.B. Duan, W.G. Chu, J. Yu, Y.C. Wang, L.N. Zhang, G.Y. Liu, J. K. Liang, G.H. Rao, Structural and magnetic properties of Zn1 − xCoxO ($0 < x < 0.30$) nanoparticles, Journal of Magnetism and Magnetic Materials 320 (2008) 1573–1581.
[12] K. Potzger, S. Zhou, Non-DMS related ferromagnetism in transition metal doped zinc oxide, Physica Status Solidi B 246 (2009) 1147–1167.
[13] N.H. Hong, J. Sakai, N. Poirot, V. Brizé, Physical Review B 73 (2006) 132404.
[14] S.D. Yoon, Y. Chen, A. Yang, T.L. Goodrich, X. Zuo, D.A. Arena, K. Ziemer, C. Vittoria, V.G. Harris, Journal of Physics: Condensed Matter 18 (2006) L355.
[15] N.H. Hong, J. Sakai, V. Brizé, Observation of ferromagnetism at room temperature in ZnO thin films, Journal of Physics: Condensed Matter 19 (2007) 036219.
[16] R. Escudero, R. Escamilla, Ferromagnetic behavior of high-purity ZnO nanoparticles, Solid State Communications 151 (2011) 97–101.
[17] T. Wangensteen, T. Dhakal, M. Merlak, P. Mukherjee, M.H. Phan, S. Chandra, H. Srikanth, S. Witanachchi, Magnetism induced by capping of non-magnetic ZnO nanoparticles, Journal of Alloys and Compounds 509 (2011) 6859–6863.
[18] J. Hong, J. Choi, S.S. Jang, J. Gu, Y. Chang, G. Wortman, R.L. Snyder, Z.L. Wang, Magnetism in dopant-free ZnO nanoplates, Nano Letters 12 (2012) 576–581.
[19] Z.B. Xia, J. Sha, Y.J. fang, Y.T. Wan, Z.L. Wang, Y.W. Wang, Purposed buit ZnO/Zn5(OH)8AC2.2H2O architetures by hydrothermal synthesis, Crystal Growth and Design 10 (2010) 2759–2765.
[20] R. Shi, P. Yang, X. Dong, Q. Ma, A. Zhang, Growth of flower-like ZnO on ZO nanorod arrays created on zin substrate through low-temperature hydrothermal synthesis, Applied Surface Science 264 (2013) 162–170.
[21] Y. Köseoğlu, H. Kavas, Size and Surface Effects on Magnetic Properties of Fe_3O_4 Nanoparticles, Journal of Nanoscience and Nanotechnology 8 (2008) 584–590.
[22] S.Y. Gao, H.J. Zhang, X.M. Wang, R.P. Deng, D.H. Sun, G.L. Zheng, ZnO-based hollow microspheres: biopolymer-assisted assemblies from ZnO nanorods, Journal of Physical Chemistry B 110 (2006) 15847–15852.
[23] Z.Q. Wang, X.D. Liu, J.F. Gong, H.B. Huang, S.L. Gu, S.G. Yang, Epitaxial growth of ZnO nanowires on ZnS nanobelts by metal organic chemical vapor deposition, Crystal Growth and Design 8 (2008) 3911–3913.
[24] J.B. Shen, H.Z. Zhuang, D.X. Wang, C.S. Xue, H. Liu, Growth and characterization of ZnO nanoporous belts, Crystal Growth and Design 9 (2009) 2187–2190.
[25] P.X. Gao, W.J. Mai, Z.L. Wang, Superelasticity and nanofracture mechanics of ZnO nanohelices, Nano Letters 6 (2006) 2536–2543.
[26] J. Qi, M. Olmedo, J.J. Ren, N. Zhan, J. Zhao, J.G. Zheng, J.L. Liu, Resistive switching in single epitaxial ZnO nano islands, ACS Nano 6 (2012) 1051–1058.
[27] F.H. Zhao, W.J. Lin, M.M. Wu, N.S. Xu, X.F. Yang, Z.R. Tian, Q. Su, Hexagonal and prismatic nanowalled ZnO microboxes, Inorganic Chemistry 45 (2006) 3256–3260.
[28] S. Li, Z.W. Li, Y.Y. Tay, J. Armellin, W. Gao, Growth mechanism and photonic behaviors of nanoporous ZnO microcheerios, Crystal Growth and Design 8 (2008) 1623–1627.
[29] A.C. Erxleben, Structures and properties of Zn(II) coordination polymers, Chemical Reviews 246 (2003) 203–228.
[30] B. Daragh, F.A. Rabie, B. Teresa, G.R. David, T. Brendan, O.H. Martin, M. Enda, Study of morphological and related properties of aligned zinc oxide nanorods grown by vapor phase transport on chemical bath deposited buffer layers, Crystal Growth and Design 11 (2011) 5378–5386.
[31] D. Byrne, E. McGlynn, K. Kumar, M. Biswas, M.O. Henry, G. Hughes, A study of drop-coated and chemical bath-deposited buffer layers for vapor phase deposition of large area, aligned, zinc oxide nanorod arrays, Crystal Growth and Design 10 (2010) 2400–2408.
[32] C. Li, G.J. Fang, F.H. Su, G.H. Li, X.G. Wu, X.Z. Zhao, Self-organized ZnO microcombs with cuboid nanobranches by simple thermal evaporation, Crystal Growth and Design 6 (2006) 2588–2591.
[33] Y. Köseoğlu, M. Bay, M. Tan, A. Baykal, H. Sözeri, R. Topkaya, N. Akdoğan, Magnetic and dielectric properties of $Mn_{0.2}Ni_{0.8}Fe_2O_4$ nanoparticles synthesized by PEG-assisted hydrothermal method, Journal of Nanoparticle Research 13 (2011) 2235–2244.
[34] Y. Köseoğlu, Structural, magnetic, electrical and dielectric properties of MnxNi1xFe2O4 spinel nanoferrites prepared by PEG assisted hydrothermal method, Ceramics International 39 (2013) 4221–4230.
[35] M. Sertkol, Y. Koseoglu, A. Baykal, H. Kavas, M.S. Toprak, Synthesis and magnetic characterization of Zn0.7Ni0.3Fe2O4 nanoparticles via microwave-assisted combustion route, Journal of Magnetism and Magnetic Materials 322 (2010) 866–871.
[36] Y. Köseoğlu, C. Durmaz, R. Yilgin, Rapid synthesis and Room temperature Ferromagnetism of Ni Doped ZnO DMS Nanoflakes, Materials Chemistry and Physics (2013) (submitted).
[37] Y. Köseoğlu, A. Baykal, F. Gözüak, H. Kavas, Structural and magnetic properties of $Co_xZn_{1-x}Fe_2O_4$ nanocrystals synthesized by microwave method, Polyhedron 28 (2009) 2887–2892.
[38] A. Manikandan, J. Judith Vijaya, L. John Kennedy, M. Bououdina, Structural, optical and magnetic properties of $Zn_{1-x}Cu_xFe_2O_4$ nanoparticles prepared by microwave combustion method, Journal of Molecular Structure 1035 (2013) 332–340.
[39] L.H. Reddy, G.K. Reddy, D. Devaiah, B.M. Reddy, A rapid microwave-assisted combustion synthesis of CuO promoted CeO_2–M_xO_y (M= Zr, La, Pr and Sm) catalysts for CO oxidation, Applied Catalysis A: General 445 (2012) 297–305.
[40] L.C. Nehru, V. Swaminathan, C. Sanjeeviraja, Rapid synthesis of nanocrystalline ZnO by a microwave-assisted combustion method, Powder Technology 226 (2012) 29–33.
[41] G. Mill, Z.G. Li, D. Meisel, Photochemistry and spectroscopy of colloidal arsenic sesquisulfide, Journal of Physical Chemistry 92 (1988) 822.
[42] C.Xu Xu, J. Dai, J. Hu, F. Li, S. Zhang, Size dependence of defect-induced room temperature ferromagnetism in undoped ZnO nanoparticles, Journal of Physical Chemistry C 116 (2012) 8813–8818.
[43] C. Zhao, Y. Huang, J. Abiade, Ferromagnetic ZnO nanoparticles prepared by pulsed laser deposition in liquid, Materials Letters 85 (2012) 164–167.
[44] R. Escudero, R. Escamilla, Ferromagnetic behavior of high purity ZnO nanoparticles, Solid State Communications 151 (2011) 97–101.
[45] Z. Yan, Y. Ma, D. Wang, Z. Gao, L. Wang, P. Yu, T. Song, Impact of annealing on morphology and ferromagnetism of ZnO nanorods, Applied Physics Letters 92 (2008) 081911.
[46] M. Venkatesan, C.B. Fitzgerald, J.G. Lunney, J.M.D. Coey, Anisotropic ferromagnetism in substituted zinc oxide, Physical Review Letters 93 (2004) 177206.
[47] J.M.D. Coey, M. Venkatesan, C.B. Fitzgerald, Donor impurity-band exchange in dilute ferromagnetic oxides, Nature Materials 4 (2005) 173.
[48] K.C. Barick, M. Aslam, V.P. Dravid, D. Bahadur, Self-Aggregation and Assembly of Size-Tuneable Transition Metal Doped ZnO Nanocrystals, Journal of Physical Chemistry C 112 (2008) 15163–15170.